行政院國家科學委員會專題研究計畫　期中進度報告

西太平洋大陸棚區衛星測高應用之改善(2/3)

計畫類別：個別型計畫
計畫編號：NSC92-2611-M-009-001-
執行期間：92 年 08 月 01 日至 93 年 07 月 31 日
執行單位：國立交通大學土木工程學系

計畫主持人：黃金維

報告類型：精簡報告

處理方式：本計畫可公開查詢

中　華　民　國 93 年 5 月 27 日

行政院國家科學委員會補助專題研究計畫 □ 成 果 報 告 ▒期中進度報告

西太平洋大陸棚區衛星測高應用之改善

計畫類別：▒ 個別型計畫　　□ 整合型計畫
計畫編號：NSC　93－2611－M－009－001－
執行期間：92 年 8 月 1 日至 93 年 7 月 31 日

計畫主持人：黃金維教授
共同主持人：
計畫參與人員：董曉軍博士、徐欣瑩同學

成果報告類型(依經費核定清單規定繳交)：■精簡報告　□完整報告

本成果報告包括以下應繳交之附件：
□赴國外出差或研習心得報告一份
□赴大陸地區出差或研習心得報告一份
□出席國際學術會議心得報告及發表之論文各一份
□國際合作研究計畫國外研究報告書一份

處理方式：除產學合作研究計畫、提升產業技術及人才培育研究計畫、列管計畫及下列情形者外，得立即公開查詢
□涉及專利或其他智慧財產權，□一年□二年後可公開查詢

執行單位：國立交通大學土木系

中　華　民　國　93　年　5 月 31 日

中、英文摘要及關鍵詞：

中文摘要

關鍵詞： 衛星測高，海潮模式

本研究旨在大幅提高衛星測高在沿岸區的應用，由”最佳化參數”的決定來改善衛星測高資料的品質，並在本研究中首度採用一種新的資料型態來推求海洋重力異常。將衛星測高重力與船測重力資料在東海以及台灣海峽兩區域作比較，本研究可獲得較 NCTU01 重力模型更小之均方根差值。

通過對東中國海地區的驗潮站資料進行分析確定了該地區海潮誤差的主要來源，半日分潮、淺水分潮和長期分潮都存在顯著的誤差需要改善。在長週期潮部分，根據測高和驗潮站資料發展了一個經驗公式可以用來模擬出大部分長週期潮能量。利用 T/P 測高資料發展了一個新的海潮模式，其在部分沿岸驗潮站的結果明顯好於 CSR4.0 和 NAO99 這二個全球海潮模式。

Abstract

Keywords: satellite altimetry, ocean tide analysis

This research aims to improve coastal applications of satellite altimetry. We improve the data quality by determining a set of “optimal parameters” and use a new data type to derive gravity anomalies. Comparison with shipborne gravity will be carried out in two test area, the East China Sea and the Taiwan Strait area. The result shows this research yields a smaller RMS differences than the NCTU01 model does.

The tidal energy at selected tide gauges in this region was first examined to see the dominant tidal constituencies; it shows the semi-diurnal, shallow water and long-period tides should be improved before used in this region. An empirical formula was developed to fit the long period tides, and it works well in most gauges. A T/P-derived model was developed and the comparison shows it is much better than NAO99 and CSR4.0 models in some coastal tide gauge.

Coastal applications of satellite altimetry: gravity anomalies and ocean tide models

Cheinway Hwang, Hsin-Ying Hsu and Xiaojung Dong
Department of Civil Engineering, National Chiao Tung University, 1001 Ta Hsueh Road, Hsinchu

1. Introduction

Gravity anomalies and ocean tide models over shallow waters are useful in many geodetic and geophysical applications. Existing methods for altimetry-gravity anomaly conversions are, e.g., the Fourier transform (FT) method with deflection of the vertical (DOV) (Sandwell and Smith, 1997), FT with sea surface height (SSH) (Andersen and Knudsen, 1998), least-squares collocation (LSC) with SSH, LSC with DOV (Hwang and Parsons, 1995). A new altimeter data type, called differenced height, will be used to derive gravity anomalies from altimetry data. Furthermore, over shallow waters, altimeter data are prone to errors caused by errors in altimeter range observations (both systematic and random) and by errors in geophysical corrections (Hwang et al., 1998). Therefore, it is important to use appropriate techniques to remove data outliers and noises. In view of this, a set of "optimal parameters" will be determined for a best performance in gravity anomaly computation.

Due to complex bottom topography and ocean circulations over shallow waters, ocean response to the tidal potential can be highly nonlinear and hence ocean tides over shallow waters are difficult to model in comparison to the open oceans. Methods for tide modeling with altimetry include, e.g., the hydrodynamic method (Lefèvre et al., 2000), the harmonic method (Andersen, 1999), and the response method (Eanes and Bettadpur, 1996). In this paper, the tidal energy at selected tide gauges over the Yellow and East China Seas will be first examined to see the dominant tidal constituencies. TOPEX/Poseidon (T/P) altimeter data will be then used to compute tidal parameters along T/P ground tracks using various methods and comparison among T/P-derived model, the NAO tide model and the CSR tide model (Eanes and Bettadpur, 1996) will be performed.

2. Coastal gravity anomalies from satellite altimetry

2.1 Altimeter data and use of differenced height

We use altimeter data from Seasat, Geosat ERS-1/GM, ERS-1, ERS-2 and TOPEX/POSEIDON missions to obtain optimal parameters for computing coastal gravity anomalies. Table 1 summarizes the missions and data characteristics. The orbits and geophysical correction models associated with these data are the most up-to-dated.

In this paper, we introduce a new data type, differenced height, which is similar to along-track deflection of the vertical (DOV) (Hwang et al., 2002), for gravity derivation. A differenced height is defined as

$$d_i = h_{i+1} - h_i \tag{1}$$

where i is index. Using differenced height has the same advantage as using along-track DOV in

terms of mitigating long wavelength errors in altimeter data. To use differenced height for gravity estimation, one may employ least-squares collocation (Moritz, 1980). First, the covariance function between two differenced heights is

$$\begin{aligned}\operatorname{cov}(d_i, d_j) &= \operatorname{cov}(h_{i+1} - h_i, h_{j+1} - h_j) \\ &= \operatorname{cov}(h_{i+1}, h_{j+1}) - \operatorname{cov}(h_{i+1}, h_j) - \operatorname{cov}(h_i, h_{j+1}) + \operatorname{cov}(h_i, h_j)\end{aligned} \quad (2)$$

The covariance function between gravity anomaly and differenced height is

$$\begin{aligned}\operatorname{cov}(\Delta g, d_i) &= \operatorname{cov}(\Delta g, h_{i+1} - h_i) \\ &= \operatorname{cov}(\Delta g, h_{i+1}) - \operatorname{cov}(\Delta g, h_i)\end{aligned}$$

Gravity anomaly is computed from differenced heights as

$$\mathbf{s} = \mathbf{C}_{\mathbf{sl}}(\mathbf{C}_{\mathbf{s}} + \mathbf{C}_{\mathbf{n}})^{-1}\mathbf{l} \quad (3)$$

where vectors **s** and **l** contain gravity anomalies and differenced heights, $\mathbf{C}_{\mathbf{s}}, \mathbf{C}_{\mathbf{s}},$ and $\mathbf{C}_{\mathbf{n}}$ are the covariance matrices for gravity anomaly-differenced height, differenced height- differenced height, and noises of differenced height, respectively; see Moritz (1980).

2.2 Determination of optimal parameters

In the gravity derivations, optimal parameters in altimeter data preprocessing and in the altimetry-gravity anomaly conversion must be determined. Consider differenced height as a time series with along-track distance as the independent variable. First, a filtered time series is obtained by convolving the original time series with the Gaussian function

$$f(x) = e^{-\frac{x^2}{\sigma^2}}$$

(2)

where σ is the 1/6 of the given window size of convolution. The definition of the Gaussian function is the same as that used in GMT (Wessel and Smith, 1995). For all data points the differences between the raw and filtered values are computed, and the standard deviation of the differences is found. The largest difference that also exceeds three times of the standard deviation is considered an outlier and the corresponding data value is removed from the time series. The cleaned time series is filtered again and the new differences are examined against the new standard deviation to remove further, possible outliers. This process stops when no outlier is found.

We choose an area near Indonesia, with the geographic borders from 5˚S to 3˚N and from 115˚E to 120˚E, as a testing area. Table 2 shows the optimal parameters and the results of comparison between altimeter-derived and shipborne gravity anomalies. Fig. 1 shows the trace of a selected ship cruise with gravity data. Fig. 2 shows ship borne gravity anomalies, as well as the altimeter derived gravity anomalies, along the ship track. Use of the optimal parameters yields smaller RMS difference in comparison to the case without such parameters.

Table 1: A summary of satellite altimeter data

Mission	Repeat period (day)	Data duration	Orbit height (km)	Inclination angle (˚)	mean track separation at the equator (km)
Seasat	no	78/08-78/11	780	108	165
Geosat/GM	no	85/03-86/09	788	108	4
Geosat/ERM	17	86/11-90/01	788	108	165
ERS1-/35d	35	92/04-93/12 95/03-96/06	781	98.5	80
ERS-1/GM	no	94/04-95/03	781	98.5	8
ERS-2/35d	35	95/04-98/10	785	98.5	80
T/P	10	92/12-00/06	1336	66	280

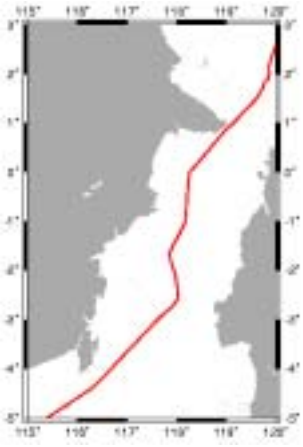

Fig 1: ship-borne gravity track

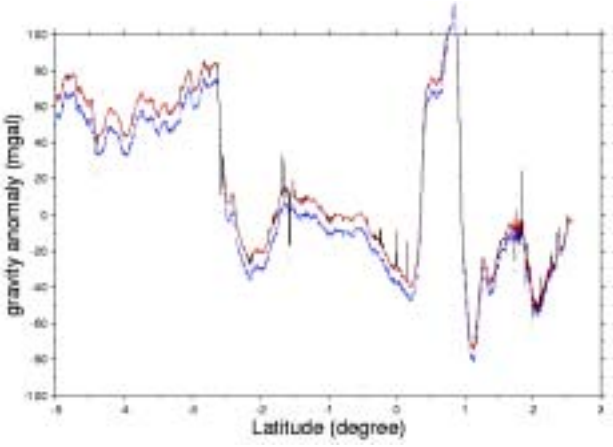

Fig 2: comparison between altimeter derived gravity (blue) and shipborne gravity (red).

Table 2: optimal parameters

Parameters description	**Raw data**	**Optimal parameters**
outlier rejection radius of non-repeat mission	3.5 km	3.5 km
filter radius of non-repeat mission	No filter	14 km
outlier rejection radius of repeat mission	3.5 km	7 km
data select window in LSC computation	30’	40’
filter on gravity anomaly	no filter	16 km
RMS between shipborne and altimeter gravity anomalies	8.63 mgal	6.65 mgal

(5)

2.3 Gravity anomalies over the Taiwan Strait and the East China Sea

Two shallow-water areas, the Taiwan Strait and the East China Sea, were chosen to experiment with the use of differenced heights and optimal parameters for gravity anomaly recovery. The shipborne gravity anomaly data are available in the two areas and they are from

Hsu et al. (1998) and the National Geophysical Data Center (NGDC). Before comparison, the ship gravity anomalies were adjusted to the satellite-derived gravity anomalies using the method described in Hwang and Parsons (1995). The ship tracks are shown in Fig. 3 and Fig 4. The results of comparisons are given in Table 3. Our comparisons indicate that the use of LSC with differenced height yields a smaller RMS differences than the method used in computing the NCTU01 model (Hwang et al., 2001) in these two regions.

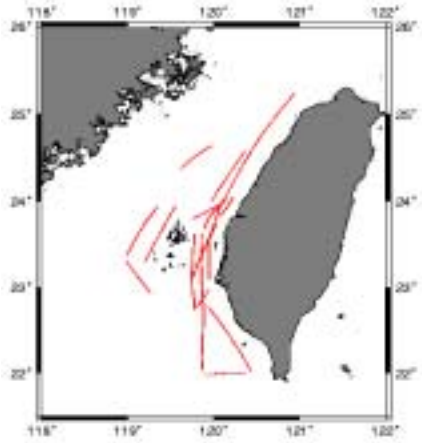

Fig 3: Distribution of shipborne gravity in anomalies in the Taiwan Strait.

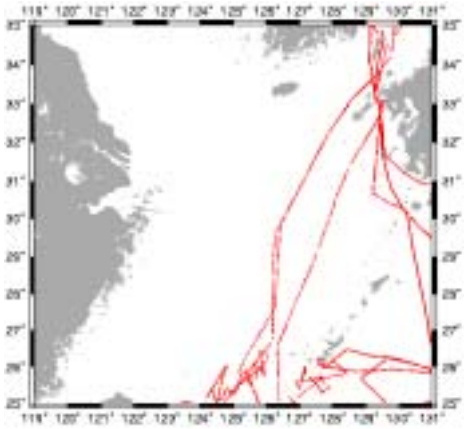

Fig 4: Distribution of shipborne gravity anomalies in the East China Sea.

Table 3: RMSdifferences (in mgals) between altimeter-derived and shipborne gravity.

Method	Taiwan	East china sea
LSC with differenced height	9.06	9.59
NCTU01	10.73	11.86

3. Shallow water ocean tides from satellite altimetry

3.1 Data and energy of tides

Another application of altimetry is tide modeling. In this paper, sea level data from T/P altimetry and 11 local tide gauges were used to model ocean tides over the Yellow Sea and East China Sea (YSECS). Typical errors of global ocean tide models are about 2 cm in the open sea, but they can be larger over YSECS due to irregular coastlines and continental shelves (Lefevre et al, 2000). We developed a local tide model using only altimeter data by along-track method. In this method, a sea surface height (SSH) series along a satellite ground track is constructed on a standard point (SP), and tidal parameters are then estimated from the SSH series at each SP using the response method. The along track tidal parameters were then interpolated to any desired locations by a method described in Sandwell (1987). The advantage of the along track method is that it does not require a spatial smoothing, which can be problematic over YSECS due to short-wavelength variations of the tidal parameters.

Sea level records from 1985 to 1995 at 11 tide gauges were analyzed to see the energy distribution in this region (see Table 4). The 11 tide gauges are evenly distributed along the coastlines of YSECS. Five tide gauges are located along the coastline of the mainland China (group A), and the rest are located along an island chain from Taiwan to the Japan mainland. At each tide gauge, energy spectra are calculated by the Fourier method based on at least 976 days continuous hourly measurements. The energy partition in Table 4 is obtained by integrating the FFT spectral densities over various frequency intervals listed at the first column of Table 4.

Table 4: Energy distribution at tide gauges (in cm^2)

	Group A					Group B					
	KM	LHT	LS	SJS	LYG	IS	KL	NG	NH	NZ	NS
>10days	156	301	250	275	309	200	165	205	113	159	204
10-1.5days	110	275	168	167	212	16	32	24	14	15	23
1.2-0.8 days*	939	497	879	879	939	455	384	701	425	335	701
0.6-0.4 days**	20272	5658	11760	11760	15300	1151	271	4156	1981	2008	4156
<0.4 days	32	7	53	53	160	2	3	5	1	1	4

* Diurnal band, ** Semi-diurnal band

KM-Kanmen, LHT-Laohutou, LS-Lusi, SJS-Shijiusuo, LYG-Lianyungang, IS-Ishigaki, KL-Keelung, NG-Nagasaki, NH-Naha, NZ-Naze, NS-Nishinoomote

Below is a summary from Table 4: (1) All semi-diurnal tides are significantly stronger than the diurnal tides, and also larger than the long period tides and shallow water tides (period short than 0.4 days). At some tide gauges, the energy in the semi-diurnal band even reaches 90% of the total energy. (2) The energy above 10 days is significant in both group A and group B, and no obvious difference in energy exists between group A and group B within this band. (3) The energy in group A is greater than Group B when the period is short than 10 days and (4) High energies also exists in the bands between 1.5 days to 10 days, and this energy is likely from storm surges.

3.2 Long-period ocean tides (LPT)

Most of LPT is affected by the weather, such as storm surges and seasonal sea temperature variability. In this study, LPT was divided into two different parts: periods longer than 10 days and shorter than 10 days. The latter are largely produced by storm surges, and the energy can reach about 200 cm^2. Because we do not have a local storm surge model, this energy cannot be analyzed further. The LPT with periods longer than 10 days include 4 constituents: Mf, Mm, SSa and Sa. Several methods can be used to improve LPT in this band: (1) use an equilibrium model, (2) use tidal constants (TC) estimated from in situ measurements within each year using the harmonic method, and then average them over a few years (1985-1995 in this study), (3) same as the previous method, but use only Sa tidal constants and (4) use an empirical formula. By comparing Sa tidal constants (amplitude A in cm and phase θ_0 in degree) and latitude (ϕ, in degree) at each tide gauge or T/P SP, linear relations can be constructed as follows:

$$A = 0.159 + 0.591\phi$$
$$\theta_0 = 217.4°$$

for tidal records,

and

$$A = -3.316 + 0.631\phi$$
$$\theta_0 = 216.6°$$

for T/P sea levels.

By averaging the above coefficients, we get

$$A = -1.729 + 0.611\phi$$
$$\theta_0 = 217°$$

The energies before and after using the above four methods are listed in Table 5. The equilibrium method is nearly not helpful to the energy improvement, because the correction is too small (only 1-2 cm). In other words, most of the LPT above 10 days are not caused by the astronomical phenomena but the weather. By comparing the correction with 4 constituents (3^{rd} row in Table 5) and Sa only (4^{th} row), the effects of Mf， Mm and SSa are very small. The numbers in 5^{th} row show the empirical formula works well in most gauges except with Kanmen (KM).

Table 5: Energy (in cm^2)of tides with periods less than 10 days at tide gauges

	Group A					Group B					
	KM	LHT	LS	SJS	LYG	IS	KL	NG	NH	NZ	NS
Before correction	156	301	250	275	309	200	165	205	113	159	204
Equilibrium model	155	301	249	275	309	201	166	205	113	160	205
Tidal Constants	69	40	62	45	57	84	22	33	48	43	33
TC (Sa only)	80	43	69	50	65	62	24	36	39	43	36
Empirical formula	123	56	68	55	71	70	35	37	38	41	38

3.3 Semi-diurnal and diurnal tides

The diurnal and semi-diurnal ocean tides can be analyzed by the harmonic method or the response method. Usually, the harmonic method was used to analyze long tidal records and the response method for shorter ones such as sea levels from altimetry. In this paper, we use: (1) the harmonic method to analyze hourly tidal records, (2) the response method to analyze hourly tidal records, (3) the response method to analyze T/P sampled (9.91564 days) sea levels, (4) the T/P derived Joint Ocean (JOT/TP) tide model from the along track method, (5) the NAO99 model (Matsumoto, 2000) and (6) the CSR4.0 ocean tide model (Eanes,1996) to derive the tidal parameters at each tide gauge and examine the remaining energy.

Table 6: Energy in the semi-diurnal band (in cm^2)

	Group A					Group B					
	KM	LHT	LS	SJS	LYG	IS	KL	NG	NH	NZ	NS
Before correction	20272	5658	11760	11760	15300	1151	271	4156	1981	2008	4156
TG constants	26	10	64	29	70	2	4	4	2	3	4
TG response	79	38	106	86	142	2	10	7	2	3	7
T/P sample	82	43	140	85	136	3	11	8	2	4	8
JOT/TP	3250	830	995	1990	3592	123	610	449	180	172	768
NAO99	427	212	1023	5063	5784	19	72	298	41	26	2165
CSR4.0	1339	1201	13009	18104	19051	24	545	167	24	19	4156

In all cases, the remaining energy after applying the response method is larger than that obtained from the harmonic method. This suggests that the assumption of tidal response to the tidal potential in this region is not quite valid. Since the difference in energy between the harmonic and response methods is cm^2 level, which is a weak energy due to storm surge, the response method is still valid here. The difference in energy between the hourly and T/P sampled records is only a few cm^2, suggesting that the T/P time series at SP provides enough sampled values for deriving the tidal parameters. Among three global ocean tide models, JOT and NAO99 seem to be more accurate than CSR4.0 over YSECS. JOT is the most accurate in group A, and NAO99 performs better than the other two models in group B. Because JOT and NAO99 use a similar technique to process altimeter data, this difference lies in the interpolation method. One explanation is that the hydrodynamic model used in the NAO99 model outperforms Sandwell's biharmonic spline interpolation method, but still performs well at some parts of YSECS costal areas. A similar method can also be used to analyze diurnal tides, but the result is not presented here.

3.4 Shallow water tides

The energy in the shallow water band is about a dozen cm^2 in group A and a few cm^2 in group B, which is not significant in comparison to the remaining energy in other frequency bands. In this study, the harmonic method is used to compute the amplitude of the main shallow water tides. A tidal amplitude of more than 5 cm is found at the Lianyungang (LYG) and Shijiusuo (SJS) tide gauge stations, and the leading constituents are M4 (both LYG and SJS) and MS4 (LYG only). In addition, amplitudes of more than 2 cm in M4 and MS4 are also found at Kanmen (KM) and Lusi (LS). Therefore, it is suggested to include the M4 and MS4 constituents for local

tide models in these areas.

4. Conclusions

Improved determinations of gravity anomalies from altimetry over shallow waters have been achieved by using differenced heights and optimal parameters. Such a procedure can be applied to the world coastal areas and the resulting coastal gravity fields will contribute to a number of geophysical studies. Ocean tides over the Yellow and China Seas are also improved over the existing global tide models, but further work in modeling tides with periods less than those of the semidiurnal tides is needed.

Acknowledgements

This research is supported by the National Science Council of ROC, under grant NSC 92-2611-M-009-001. This is also a contribution to the IAG Special Study Groups 3.186 and 2.3.

References

Andersen O (1999) Shallow water tides in the northwest European shelf region from TOPEX/POSEIDON altimetry. J Geophys Res 104 (C4): 7729-7741

Andersen O, Knudsen P (1998) Global marine gravity from the ERS-1 and Geosat geodetic mission altimetry. J Geophys Res 103: 8129-8137

Eanes R, Bettadpur S (1996) The CSR 3.0 global ocean tide model, Center for Space Research, Technical Memorandum. CSR-TM-96-05, The University of Texas Center for Space Research, Austin, Texas

Hsu S, Liu C, Shyu C, Liu S, Sibue J, Lallemand S, Wang C, Reed D (1998) New gravity and Magnetic Anomaly Maps in the Taiwan-Luzon region and their preliminary interpretation. TAO 9(3): 509-532

Hwang C, Parsons B (1995) Gravity anomalies derived from Seasat, Geosat, ERS-1 and Topex/Poseidon altimeter and ship gravity: a case study over the Reykjanes Ridge. Geophys J Int 122: 551-568

Hwang C, Kao EC, Parsons B (1998) Global derivation of marine gravity anomalies from Seasat, Geosat, ERS-1 and TOPEX/POSEIDON altimeter data. Geophys J Int 34: 449-460

Hwang C, Hsu HY, Jang R (2002) Global mean sea surface and marine gravity anomaly from multi-satellite altimetry: applications of deflection-geoid and inverse Vening Meinesz formulae. J Geod 76: 407-418

Lefèvre F, Provost CL, Lyard FH (2000) How can we improve a global ocean tide model at a regional scale? a test on the Yellow Sea and the East China Sea. J Geophys Res 105(C4): 8707-8725

Matsumoto K, Takanezawa T, Ooe M (2000) Ocean Tide Models Developed by Assimilating TOPEX/POSEIDON Altimeter Data into Hydrodynamic Model: A Global Model and a Regional Model Around Japan. J Oceanogr 56: 567-581

Moritz H (1980) Advanced Physical Geodesy. Herbert Wichmann, Karlsruhe

Sandwell DT (1987) Biharmonic spline interpolation of GEOS-3 and SEASAT altimeter data. Geophys Res Lett 2: 139-142

Sandwell DT, Smith WHF (1997) Marine Gravity Anomaly from Geosat and ERS-1 Satellite Altimetry. J Geophys Res 12: 10039-10054

Wessel P, Smith WHF (1995) New version Generic Mapping Tools release. EOS Trans, AGU